2-D Imaging of CF_2 Density by Laser-Induced Fluorescence of CF_4 Etching Plasmas in the GEC rf Reference Cell

Brian K. McMillin and Michael R. Zachariah

Chemical Science and Technology Laboratory
National Institute of Standards & Technology, Gaithersburg, MD 20899

ABSTRACT

Spatially resolved 2-D maps of the relative CF_2 density in low-pressure rf $Ar/CF_4/O_2$ discharges generated within a parallel-plate Gaseous Electronics Conference reference reactor have been obtained using planar laser-induced fluorescence imaging. The present experiments cover a wide range of pressure, composition, flowrate, and power deposition conditions (13.3-133.3 Pa, 1-100% CF_4, 1-10% O_2, 5-100 sccm, 3-35 W) and, where possible, the results are compared to previous studies reported in the literature. In general, varying the pressure led to significant changes in both the magnitude and spatial distribution of CF_2 density, while varying the composition, flowrate, and power primarily affected only the magnitude of the CF_2 density.

INTRODUCTION

Low-pressure radio-frequency (rf) plasma etching of silicon and silicon dioxide with CF_4-based chemistries is used extensively during the manufacturing of microelectronic integrated circuits. Despite their widespread use, the physical and chemical phenomena which determine the behavior and the resulting etching performance of these plasmas are not fully understood. With regard to the gas-phase chemistry, for example, a great deal of experimental[1] and, to a lesser extent, modeling research[2] has been conducted to improve the understanding of these plasmas, but detailed comparisons between modeling and experiment have been limited. Species measurements have been made by a number of techniques, but typically these have been limited to 1-D spatial profiles or single-point (line-of-sight) measurements at the plasma center. As 2-D modeling becomes more widespread, a more extensive experimental data base will be necessary for benchmarking and verification of these plasma chemistry models.

In previous studies, we used planar laser-induced fluorescence (PLIF) imaging to map the argon metastable density field in low-pressure argon and argon/molecular discharges.[3-4] The purpose of this study is to extend those PLIF measurements to map the spatially resolved, 2-D CF_2 density field in $Ar/CF_4/O_2$ etching plasmas generated within a Gaseous Electronics Conference (GEC) rf reference cell.[5] The CF_2 radical is an important species in CF_4 etching plasmas because it influences the balance between polymer deposition and etching of silicon and/or silicon dioxide.[1] As a result, a number

of previous experimental studies have reported single-point, line-of-sight, or 1-D profile measurements of CF_2 density using mass spectrometry,[6] infrared diode laser-absorption,[7] and laser-induced fluorescence,[8] but, to our knowledge, the present results are the first complete 2-D measurements of CF_2 density in any reactor. These measurements are of interest because they provide additional insight into the plasma uniformity through 2-D visualization of the relative CF_2 density, and because they are a useful data source for model validations.

EXPERIMENTAL DETAILS

The experiments were conducted using a capacitively-coupled, parallel-plate, asymmetrically driven GEC cell, which has been described in detail previously[5] and is shown schematically in Fig. 1. Briefly, the stainless steel reactor used here has 10.2 cm diameter aluminum water-cooled electrodes with a 2.25 cm separation. The lower electrode was powered with a 13.56 MHz supply coupled through a matching network and isolating rf filter. The upper electrode and the chamber were grounded. The feed gas mixture was delivered through the upper electrode via a showerhead arrangement of holes and pumped out through a feedback-controlled throttle valve using a mechanical pump. The flowrate was varied over 5-100 sccm and the pressure was varied over 13.3-133.3 Pa (100-1000 mTorr). Voltage and current waveforms were measured at the base of the powered electrode, stored with a digital oscilloscope, and Fourier-analyzed to determine the actual power delivered to the plasma.

Spatially resolved 2-D images of CF_2 relative concentration were obtained using PLIF imaging. A quadrupled Nd:YAG laser sheet (266 nm, 10 ns, ~0.3 mJ, ~1 cm^{-1}, 5 mm × 25 mm) was used to illuminate the central vertical plane of the discharge and excite transitions in the A(0,2,0)←X(0,1,0) band of CF_2 (see Fig. 1). The resulting broadband laser-induced fluorescence (300-400 nm) was imaged at a 90° angle to the illumination plane with an intensifier-gated, cooled CCD camera using an f/4.5 lens. The imaged region included approximately one-half of the discharge, extending from the centerline to ~1 cm beyond the edge of the electrodes. A 300 nm long-pass filter was used to reject laser scattering and a colored-glass filter was used to reduce the visible plasma emission reaching the camera. The CF_2 fluorescence images were obtained by temporally averaging over ~1000 laser shots with an ~300 ns intensifier gate width and spatially averaging over 2×2 pixels to improve the signal-to-noise ratio.

To reduce the data, the raw fluorescence images were corrected as detailed previously;[3] however, no corrections for fluorescence yield were necessary here, because, as in previous studies,[9] no significant differences in the fluorescence decay time were observed for the conditions examined. In addition, to relate the fluorescence signal to the CF_2 density, the neutral gas temperature was assumed to be uniform, rotationally and vibrationally equilibrated, and constant for all conditions examined; i.e., we assumed the concentration of the laser-probed states inferred from the fluorescence measurement perfectly tracks the total CF_2 density.

RESULTS AND DISCUSSION

Relative 2-D measurements of the CF_2 density distribution were obtained in $Ar/CF_4/O_2$ rf discharges over a wide range of pressure, composition, flowrate, and power deposition conditions (13.3-133 Pa, 1-100% CF_4, 1-10% O_2, 5-100 sccm, 3-35 W). While the

absolute CF_2 density was not determined in these experiments, a recent investigation using a GEC cell[10] reported CF_2 densities of ~10^{12}-10^{13} cm^{-3} at similar conditions. Generally speaking, in the present experiments, varying the pressure led to significant changes in both the magnitude and spatial distribution of CF_2 density, while varying the composition, flowrate, and power primarily only affected the magnitude of the CF_2 density.

Figure 2 shows contour plots of the spatial distribution of CF_2 density in 75%CF_4/Ar discharges at constant power (12 W) and flowrate (10 sccm) and four pressures, ranging from 13.3 to 133.3 Pa (100-1000 mTorr). In these plots, the z=0 and z=2.25 cm locations correspond to the powered and grounded electrodes, respectively. As observed in previous GEC cell experiments,[3,4] significant radial variations in species concentration are observed. The peak CF_2 density typically occurs at r~3-5 cm, presumably because of an enhanced electric field near the edge of the powered electrode, which leads to increased excitation and dissociation. This increased excitation near the edge of the powered electrode is most apparent for the 33.3 and 66.6 Pa cases. Interestingly, the peak CF_2 concentration for the 13.3 and 133.3 Pa cases occurs within the plasma bulk, although the latter case shows high concentration contours emanating from the edge of the powered electrode.

In all cases, the centerline (r=0) axial distribution of CF_2 density is relatively symmetric, with the peak occurring near the center of the discharge (z~1 cm). This axial distribution is primarily the result of the CF_2 production profile, which is dominated[11] by the high energy electron impact reaction $e+CF_4 \rightarrow CF_2+2F+e$ (threshold ~13 eV). This is evidenced to some extent by its similarity to the argon emission profile at similar conditions,[4] since the argon excitation threshold (~14 eV) and cross-section energy dependence (over ~12-30 eV) are similar to that of the CF_4 electron impact reaction noted above (see, for example, Refs. 12-13). The CF_2 profile is, of course, also affected by diffusion, since CF_2 is a relatively long-lived species, and by destruction mechanisms such as heterogeneous (wall recombination) and gas-phase recombination reactions.[14]

Figures 3-5 show the dependence of the CF_2 density on power and feed gas composition at constant pressure (66.7 Pa) and flowrate (25 sccm). In these cases, large changes in the *magnitude* of the CF_2 density were observed as power and composition were varied, but the *spatial distribution* was not significantly affected. Hence, because of space limitations, we simply show the image-averaged CF_2 density as a function of power and composition to illustrate the changes in the discharge.

As indicated in Fig. 3, the CF_2 concentration increases with power, as expected, since higher powers should lead to more CF_4 dissociation. The CF_2 density increases in an essentially linear fashion over the conditions examined here, but with a slope of less than unity; i.e., the $[CF_2]$ increases by ~6× as the power is increased by ~10×. This trend is consistent with that reported by Pang and Brueck,[9] although the present measurements show about a 20% weaker slope. The relatively weak slope in Fig. 3 is not too surprising, since some of the increased power goes into ion bombardment as well as into the formation of CF_3 and CF through additional electron impact reactions.

The effect of argon diluent on the CF_2 concentration is shown in Fig. 4. As the CF_4 concentration is increased from 1-100%, the CF_2 concentration increases linearly by about 2.5×. This relatively small increase in CF_2 concentration suggests that very little of the

CF_4 is dissociated in the pure CF_4 discharge at these conditions. For example, even if all of the CF_4 is dissociated for the most dilute (1.2% CF_4) case, the degree of dissociation for the pure CF_4 case can only be 2-3%, since the primary fragments in the electron impact dissociation of CF_4 are CF_2 and CF_3 in a ~2.5:1 ratio.[11] This relatively weak increase in the CF_2 concentration (and thus CF_4 dissociation) as the argon dilution is decreased may be due to the cooling of the high energy tail in the electron energy distribution and/or a decreased electron number density resulting from additional electron attachment by CF_4.

In Fig. 5, the effect of the addition of O_2 on the CF_2 concentration in the discharge is shown. For these cases, the power was held constant at 20 W, and the CF_4 mole fraction and total flowrate were held constant at 75% and 25 sccm, respectively. It is well established that the addition of only a few percent O_2 reduces the CF_2 concentration substantially, due to oxidation reactions such as $CF_2+O \rightarrow COF+F$ and $CF_2+O \rightarrow CO+2F$.[11] Here we observe a reduction in CF_2 density of about 2.5×, with an oxygen feed gas mole fraction of only 10%, which is in good agreement with the results of Pang and Brueck [9].

Figure 6 shows the effect of flowrate on the CF_2 density in an rf discharge at a constant power (20 W), feed gas composition (25% CF_4/Ar), and pressure (66.7 Pa). In varying the flowrate over 5-100 sccm, the residence time for the gas within the volume between the electrodes was decreased from ~1.5 to ~0.07 seconds. This resulted in some noticeable changes in the spatial distribution of CF_2 density, typically leading to an enhanced CF_2 concentration near the edge of the powered electrode with respect to the center of the discharge. Here again because of space limitations, however, we simply report the image-averaged CF_2 density to illustrate the effect of flowrate on the discharge.

As shown in Fig. 6, at low flowrates (high residence time) the CF_2 concentration initially increases, but further increases in flowrate (shorter residence times) result in a subsequent decrease in CF_2 concentration. Because the CF_2 production rate likely remains essentially constant (the electron number density and temperature are approximately constant and the CF_4 is largely undissociated), these changes in the concentration of CF_2 with flowrate suggest a competition among its various loss processes, which include convection, gas-phase recombination, surface losses, and diffusion. While further modeling and experiments are necessary to be certain, this variation in CF_2 concentration with flowrate might be explained as follows. At moderately high flowrates (i.e., 25 sccm) further increases in the flowrate yield a decrease in the accumulation of CF_2 within the discharge, because the dissociation products are convected away more rapidly. As the flowrate is reduced (from say 50 sccm), initially the CF_2 concentration increases because of reduced convective losses. While convection becomes less important, the primary CF_2 gas-phase recombination reaction,[11] $CF_2+F+M \rightarrow CF_3+M$, becomes somewhat more important since the CF_2 (and F) concentration increases. The CF_2 surface losses also increase because diffusive transport becomes increasingly important at lower flowrates. As the flowrate is further reduced, though, the observed decrease in CF_2 concentration cannot be attributed to increased gas-phase recombination, because that rate only depends on the (decreasing) CF_2 and F concentration. Consequently, the observed decrease in CF_2 concentration at very low flows is attributed to an increased loss due to diffusion, either by surface losses or by transport out of the imaged region. Such an increase in the contribution of diffusion and

surface recombination reactions at low flowrates has been indicated in previous modeling of F-atom concentration in CF_4/O_2 plasmas.[15]

CONCLUDING REMARKS

In this experimental study, we have used planar laser-induced fluorescence imaging to measure spatially resolved 2-D maps of CF_2 density in low-pressure rf $Ar/CF_4/O_2$ discharges generated within a GEC reference cell. In general, varying the pressure led to significant changes in both the magnitude and spatial distribution of CF_2 density, while varying the composition, flowrate, and power primarily only affected the magnitude of the CF_2 density. In all cases, significant radial variations in CF_2 density were observed (as much as 300%) with the peak density occurring near the edge of the discharge region, while the centerline axial CF_2 distribution was symmetric with the local peak occurring near the center of the electrode gap. Based on plots of the image-averaged CF_2 concentration, for the conditions examined here, the CF_2 density increased linearly with power and CF_4 mole fraction in Ar/CF_4 discharges; the dissociation fraction in mildly diluted CF_4 discharges was less than a few percent; and the CF_2 density decreased substantially with the addition of oxygen. In addition, the CF_2 density was also found to depend upon flowrate, which is attributed to changes in the various loss rates for CF_2, because, for these cases, the production rate is believed to remain essentially constant.

ACKNOWLEDGEMENTS

The authors are grateful for helpful discussions with J.K. Olthoff and M.J. Kushner. B.K. McMillin was supported as an NRC postdoctoral research associate during the course of these experiments.

REFERENCES

1. *Plasma Etching. An Introduction*, edited by D.M. Manos and D.L. Flamm (Academic Press, Boston 1989).
2. e.g., M. Dalvie and K.F. Jensen, *J. Electrochem. Soc.* **137** (4), 1062 (1990).
3. B.K. McMillin and M.R. Zachariah, *J. Appl. Phys.* (in press).
4. B.K. McMillin and M.R. Zachariah, *J. Appl. Phys.* (submitted June 1995).
5. P.J. Hargis, Jr. et al., *Rev. Sci. Instrum.* **65** (1), 140 (1994).
6. e.g., Y. Hikosaka and H. Sugai, *Jpn. J. Appl. Phys.* **32** (6B), 3040 (1993).
7. e.g., H. C. Sun, V. Patel, E.A. Whittaker, B. Singh, and J.H. Thomas III, *J. Vac. Sci. Technol. A* **11** (4), 1193 (1993).
8. S.G. Hansen, G. Luckman, G.C. Nieman, and S.D. Colson, *J. Appl. Phys.* **68** (5), 2013 (1990), and references therein.
9. S. Pang and S.R.J. Brueck, Mat. Res. Soc. Symp. Proc. **17**, 161 (1983).
10. D.B. Oh, A.C. Stanton, H.M. Anderson, and M.P. Splichal, *J. Vac. Sci. Technol. A* (to appear).
11. I.C. Plumb and K.R. Ryan, *Plasma. Chem. Plasma. Proc.* **6** (3), 205 (1986).
12. K. Tachibana, *Phys. Rev. A* **34** (2), 1007 (1986).
13. W.L. Morgan, *Plasma Chem. Plasma Proc.* **12** (4), 477 (1992).
14. J.P. Booth, G. Hancock, N.D. Perry, and M.J. Toogood, *J. Appl. Phys.* **66** (11), 5251 (1989).
15. M. Dalvie and K.F. Jensen, *J. Vac. Sci. Technol. A* **8** (3), 1648 (1990).

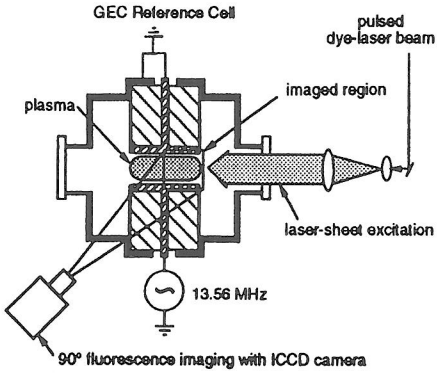

Fig. 1. Schematic diagram of the reactor and PLIF imaging setup.

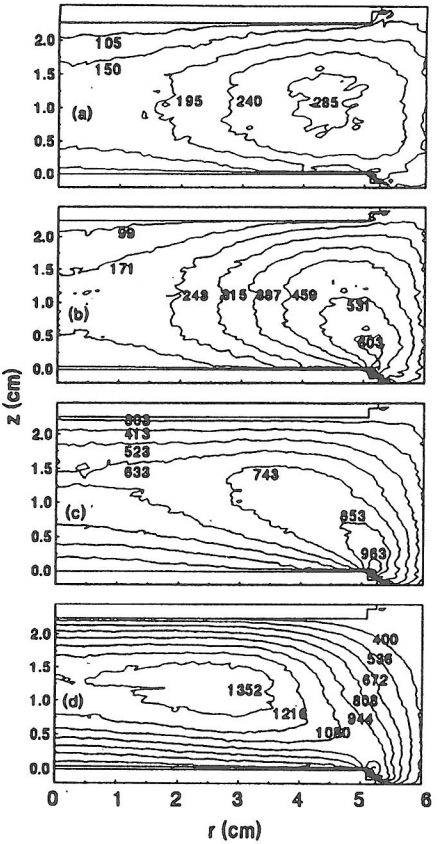

Fig. 2. Spatially resolved 2-D relative CF_2 density in a 75%CF_4/Ar discharge at (a) 13.3 Pa, (b) 33.3 Pa, (c) 66.7 Pa, and (d) 133.3 Pa.

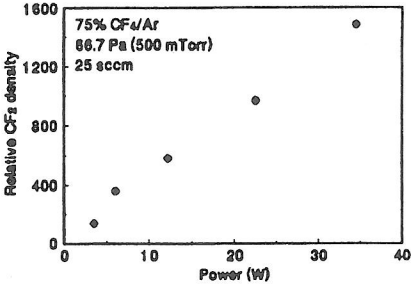

Fig. 3. Image-averaged CF_2 density as a function of power deposited in a CF_4/Ar discharge.

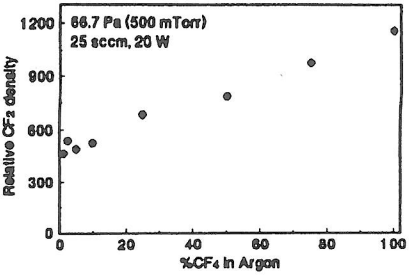

Fig. 4. Image-averaged CF_2 density as a function of argon diluent in a CF_4/Ar discharge.

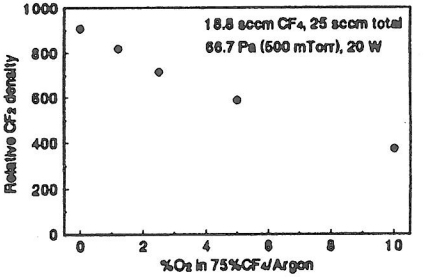

Fig. 5. Image-averaged CF_2 density vs. percentage of added O_2 to a 75%CF_4/Ar discharge.

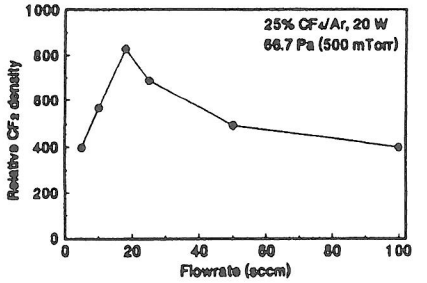

Fig. 6. Image-averaged CF_2 density as a function of flowrate in a 25%CF_4/Ar discharge.